Electroactive Cell Surfaces

DOI: 10.1002/anie.201404099

Cell-Surface Engineering by a Conjugation-and-Release Approach Based on the Formation and Cleavage of Oxime Linkages upon Mild Electrochemical Oxidation and Reduction**

*Abigail Pulsipher, Debjit Dutta, Wei Luo, and Muhammad N. Yousaf**

Abstract: *We report a strategy to rewire cell surfaces for the dynamic control of ligand composition on cell membranes and the modulation of cell–cell interactions to generate three-dimensional (3D) tissue structures applied to stem-cell differentiation, cell-surface tailoring, and tissue engineering. We tailored cell surfaces with bioorthogonal chemical groups on the basis of a liposome-fusion and -delivery method to create dynamic, electroactive, and switchable cell-tissue assemblies through chemistry involving chemoselective conjugation and release. Each step to modify the cell surface: activation, conjugation, release, and regeneration, can be monitored and modulated by noninvasive, label-free analytical techniques. We demonstrate the utility of this methodology by the conjugation and release of small molecules to and from cell surfaces and by the generation of 3D coculture spheroids and multilayered cell tissues that can be programmed to undergo assembly and disassembly on demand.*

The control of cell–cell interactions and cellular architecture in three-dimensional (3D) space and time is critical for the proper development[1] and survival of higher-order organisms.[2] These dynamic interactions are complex but essential for correct cell behavior and tissue function based on a myriad of physical, mechanical, and hydroynamic forces, as well as autocrine and paracrine signaling.[3] However, the reproduction of these processes in vitro while maintaining these dynamic and discrete cell–cell contacts is difficult and requires a multidisciplinary coordinated effort.[4] Thus, the ability to modulate cell–cell interactions in space and time would allow unprecedented control of cell behavior and enable the design of new useful dynamic tissue-engineering scaffolds, in vivo imaging systems, high-throughput tissue-based screening assays, and drug-delivery therapies.[5]

Several approaches to generate coculture tissue structures in two and three dimensions (2D and 3D, respectively) have been developed and employed, including dielectrophoresis,[6] microfabrication,[7] hydrogel,[8] and cell-patterning techniques.[9] The tailoring of cell membranes by cell-surface engineering methods has also proven to be important for the development of coculture and multicellular microtissues.[10] In particular, the integration of bioorthogonal chemical strategies[11] with cell surfaces may enable a range of cell-surface modifications for the control of ligand presentation and density, and potentially the spatiotemporal control of cell–cell interactions. Bioorthogonal chemical reactions (e.g. Diels–Alder reaction, oxime reaction, Huisgen cycloaddition, Staudinger reaction) have been extensively developed and utilized owing to their ability to be performed under physiological conditions without side reactions and in complex protein mixtures, in cell lysates, and in vivo. Furthermore, these chemistries have been applied in many fundamental cell studies,[12] drug-delivery therapies,[13] and diagnostic measuring applications.[14] However, the incorporation of a range of these chemical groups on the cell surface of a variety of cell types remains challenging.[15]

Synthetic liposomes and fused liposomes have proven very useful for numerous studies as cell-membrane model systems and as microarray platforms for the study of cell-membrane dynamics and for biotechnology applications.[16] Methods for liposome-to-liposome and liposome-to-cell fusion have also been developed for the delivery of therapeutic agents to cells and organelles, and for the study of cellular interactions.[17] However, until now, there has been no report on the use of liposome–cell fusion to deliver switchable and bioorthogonal groups directly to cell surfaces for subsequent chemoselective conjugation and the release of ligands or for the temporal programming of controlled cell–cell assembly. A strategy that combines cell-surface modification, without the use of molecular-biology techniques or biomolecules, with a stable, dynamic, and switchable bioorthogonal approach to ligand conjugation and release to direct tissue formation and subsequent disassembly would greatly benefit fundamental cell-behavioral studies and tissue-engineering research.

Herein, we report a liposome-based methodology to tailor cell surfaces with dynamic and switchable bioorthogonal chemical functionalities and to direct the assembly and disassembly of 3D tissues for applications in stem-cell differentiation and tissue engineering. We show that this strategy is redox-responsive and allows for multiple rounds of the controlled conjugation and release of molecules to and from cell surfaces in situ. This chemical methodology can be used simultaneously as an analytical probe for monitoring cellular

[*] A. Pulsipher, D. Dutta, W. Luo, Prof. M. N. Yousaf
Department of Chemistry
University of North Carolina at Chapel Hill (USA)
and
Department of Chemistry and Biology, York University (Canada)
E-mail: chrchem@yorku.ca

[**] This research was supported by the Carolina Center for Cancer Nanotechnology Excellence (NCI), the Burroughs Wellcome Foundation (Interface Career Award), the National Science Foundation (Career Award), the National Science and Engineering Research Council of Canada (NSERC), and the Canadian Foundation for Innovation (CFI).

Supporting information for this article is available on the WWW under http://dx.doi.org/10.1002/anie.201404099.

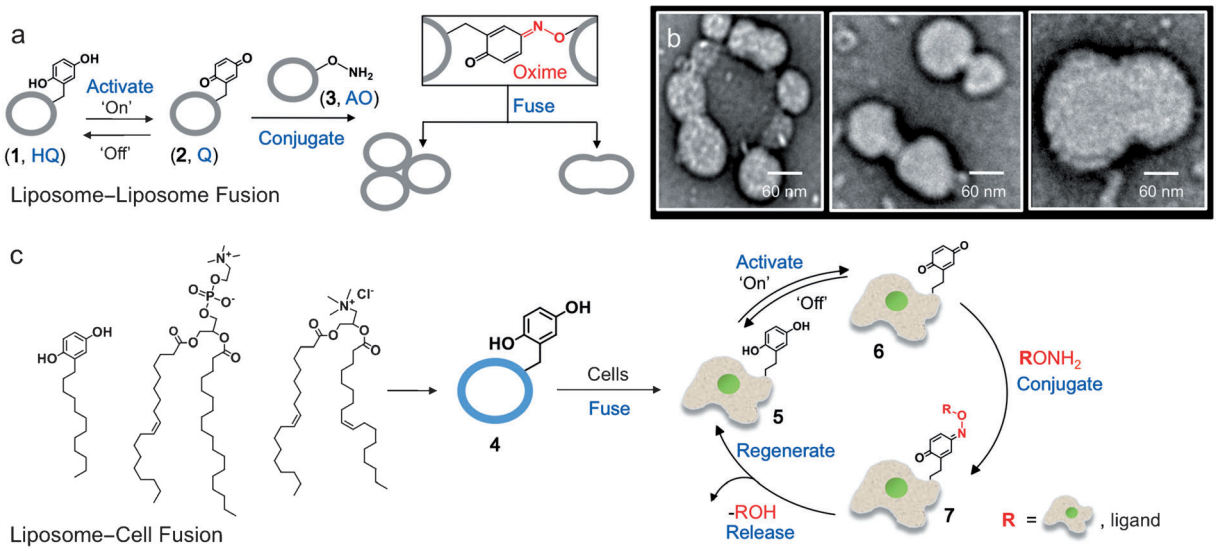

Figure 1. Scheme and transmission electron micrographs showing dynamic liposome–liposome fusion and liposome–cell fusion for tailoring cell surfaces. a) Hydroquinone (HQ)-containing liposomes **1** are in the "off state". They are activated to the "on-state" quinone (Q) **2** by mild chemical oxidation and mixed with aminooxy (AO)-containing liposomes **3**. The mixing of these two populations results in the formation (driven by oxime-bond formation) of b) multiadherent (left), partially fused (middle), and completely fused liposomal structures (right). c) General scheme for the dynamic control of cell surfaces on the basis of liposome–cell fusion for the delivery and tailoring of bioorthogonal groups. POPC, DOTAP, and a HQ-functionalized alkane are mixed to form liposomes. The addition of the resulting HQ-tethered liposomes **4** to cells in culture leads to fusion and the subsequent presentation of HQ groups on the cell surface (in **5**). HQ is then activated to Q (in **6**), which reacts chemoselectively with a range of AO-tethered (or $RONH_2$-tethered) ligands or cells to form a covalent and stable oxime linkage (in **7**). Upon a mild change in the redox environment, the oxime bond is cleaved to release the ligand or cell, and the HQ-presenting cell **5** is regenerated for subsequent rounds of dynamic and controlled conjugation and release.

interactions, as well as a trigger to alter cell-surface ligands and cell–cell contacts.

To deliver and tailor cell surfaces with dynamic and bioorthogonal chemical groups for cell-membrane manipulation and the control of cell–cell interactions, we first developed a liposome-fusion-based model system. Hydroquinone (HQ) and aminooxy (AO) alkanes were synthesized and incorporated into liposomes (see Figures S1–S5 in the Supporting Information). We have previously shown in solution and on conducting substrates how HQ is in the "off state" and can be activated to the "on-state" quinone (Q) by mild chemical or electrochemical oxidation.[18] Q can then chemoselectively react with AO-tethered ligands to form stable oxime linkages under physiological conditions (see Figure S1). The oxime linkage can then be selectively cleaved under reductive conditions to regenerate HQ with simultaneous release of the AO-tethered groups. This redox-active, oxime-based conjugation-and-release chemistry is bioorthogonal and can be carried out in complex protein mixtures, cell lysates, and cell culture.[18] Our rationale was to combine this dynamic, switchable, and bioorthogonal conjugation-and-release strategy with liposome fusion to tailor cell surfaces in vitro for studies in cell-surface manipulation and tissue engineering.

To evaluate whether liposome-to-liposome adhesion can occur through oxime chemistry, we activated HQ- to Q-containing liposomes (**1**→**2**) and then mixed them with AO-containing liposomes **3** (see Figure S5). We observed rapid liposome aggregation and fusion (Figure 1a), as shown by transimission electron microscopy (TEM) image analysis (Figure 1b). We found that over time, an oxime-driven process directed liposomes to first aggregate and then fuse to form larger assemblies (Figure 1b). We used fluorescence resonance energy transfer (FRET) to characterize liposome adhesion and observed a clear FRET signal only when the complementary oxime pair was present in the liposomes (see Figure S6). Furthermore, dynamic light scattering (DLS) showed spontaneous liposomal growth due to this oxime-driven liposomal fusion (see Figure S7). Aggregated or fused liposomal structures were not observed in control experiments in which HQ-containing liposomes were not activated or when either member of the oxime pair was missing.

We aimed to employ a similar strategy to generate electroactive, dynamic, and switchable cell surfaces. Therefore, we applied our liposome method to deliver the bioorthogonal HQ (in **4**) and AO groups (in **12**) for subsequent fusion and presentation on cell membranes. For these studies, an HQ alkane was mixed with 1-palmitoyl-2-oleoylphosphatidylcholine (POPC) and DOTAP (a cationic lipid: *N*-[1-(2,3-dioleoyloxy)propyl]-*N*,*N*,*N*-trimethylammonium) in a 10:88:2 ratio, and an AO alkane was mixed with POPC and DOTAP (5:93:2; see Figure S5). After their addition to cells (Swiss 3T3 fibroblasts (Fbs)) in culture, the liposomes first fuse, thus delivering the chemical groups to cell surfaces (Figure 1c). HQ can then be activated to generate Q, which will conjugate chemoselectively with AO-tethered ligands or cells to form a stable, interfacial oxime linkage. The oxime bond at the cell membrane can then be selectively cleaved with the simultaneous release of the ligand or cell to regenerate the HQ-presenting cell. This

dynamic cycle is noncytotoxic (see Figure S8), redox-triggered, and switchable (see Figure S1), can be performed in situ and under physiological conditions, and provides unprecedented control of cell–cell and cell–membrane interactions through the conjugation and release of ligands and cells.

Figure 2 demonstrates the dynamic and switchable conjugation and release of ligands to and from the cell membrane. After HQ-containing liposomes **4** were fused with Fbs to give **5** on a conductive substrate, cyclic voltammetry (CV) was performed, and distinct HQ-to-Q redox peaks were observed (Figure 2b). Upon activation to Q (in **6**; 400 mV, 10 s) and the conjugation of AO-tethered rhodamine to cells (conjugates **7** and **8**), a shift in the CV peaks, characterisitic of oxime formation,[19] was observed. The rhodamine-labeled Fbs were also imaged, and red fluorescence was observed (Figure 2c). Upon the application of a noncytotoxic, reductive potential (−100 mV, 10 s; see Figure S10), rhodamine was released from the cells, and HQ was regenerated on the cell surface, as indicated by CV and fluorescence microscopy (Figure 2d). We then reactivated the HQ-presenting Fbs to Q-presenting **6**, to which we conjugated biotin hydrazide, followed by fluorescein isothiocyanate (FITC)–streptavidin. We found that the cells could once again conjugate and release molecules from the cell surface, as shown by CV and fluorescence microscopy (Figure 2e). The oxime linkage is stable, and only upon the application of a mild reductive potential does the oxime cleave and release ligands.[19] In general, this dynamic strategy can be used for controlling the chemical structure of cell surfaces in 3D space and time with micro- or nanoelectrode arrays, whereby the cell-surface ligands can be replaced with any biomolecule of interest, thus creating a new tool for the modulation of cell interactions.

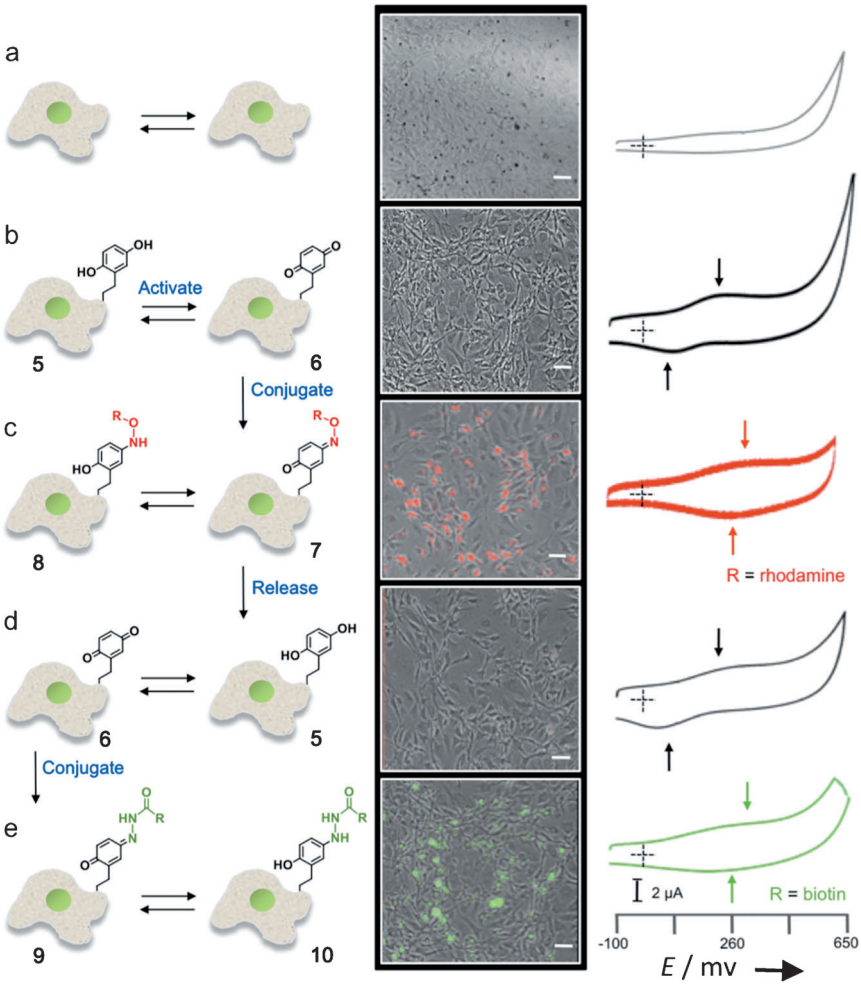

Figure 2. Electrochemical characterization of cyclical cell-surface tailoring and the release of ligands on the basis of redox-responsive chemoselective chemistry. a) Fibroblasts (Fbs) not fused with liposomes presenting HQ groups show no redox signal or fluorescence. b) HQ-containing liposomes **4** are added to Fbs, thus resulting in membrane fusion (to give **5**) and the presentation of HQ on the surface. Interconversion of stable HQ (in **5**) into Q (in **6**) can be monitored by cyclic voltammetry (CV) owing to its diagnostic redox peaks (black trace, HQ: 130 mV, Q: 258 mV). c) Activated Q-presenting Fbs **6** undergo chemoselective reaction with rhodamine–AO for cell-surface tailoring (**7** and **8**). This reaction results in stable, fluorescently labeled cells (red) and a diagnostic shift in the redox signal (red trace, HQ: 252 mv, Q: 284 mV). d) In a reductive environment, the oxime bond is cleaved with the release of rhodamine and the regeneration of HQ-presenting Fbs **5**, as indicated by a loss of fluorescence and the redox peaks of the HQ-to-Q cycle (black trace). e) Cell surfaces be conjugated a second time with hydrazide-tethered biotin (**9** and **10**) and fluorescein-presenting streptavidin, thus resulting in fluorescently labeled cells (green) and a shift in the redox peaks (green trace).

Several assays were performed to evaluate cell viability as a function of applied redox potential (see Figure S10). No change in cell viability was observed after the application of different electrochemical potentials (−100 to 650 mV, 10 s) to cells cultured with HQ for up to 7 days. From other control experiments, we could conclude that the removal of either HQ or AO from the fusion liposomes resulted in no ligand conjugation at the cell surface. When an AO alkane or HQ alkane was added directly (not in liposome form) to cells in culture, no incorporation of AO or HQ groups on the cell surface was observed. Furthermore, when chemical or electrochemical activation did not occur, the conjugation and release of ligands was not observed. We determined the amount of HQ molecules at the cell membrane upon initial liposome fusion by fluoresence-activated cell sorting (FACS). FACS analysis also demonstrated that HQ remains incorporated in the membrane after several rounds of cell growth and division, and that HQ can still be actived for the conjugation and release of ligands (see Figure S9). These results may lead to new ways to tailor and monitor in vitro and in vivo events that occur at cell membranes and may enable the develop-

ment of new types of pulse-and-chase-type experiments for cell imaging and for tracking cell movement.[20]

We further investigated the incorporation and utility of HQ on the cell surface by attaching cells to an AO-patterned substrate and releasing them again (Figure 3a). HQ-presenting Fbs **5** were activated to Q (in **6**) and then seeded onto an inert substrate presenting AO groups.[21] The Q groups on the cell surface (in **6**) reacted biospecifically with the patterned AO ligands to form an interfacial oxime linkage. The cells attached and then proliferated to fill out the patterned regions. An electrochemical trigger was then applied to cleave the oxime linkage, and cells were released from the substrate. A novel method for MALDI mass spectrometry analysis of cell-membrane incorporation showed oxime conjugation between Q-presenting cells and AO-terminated surfaces (see Figure S11).[22] This strategy enables spatial and temporal control of cell interactions in 2D and may be extended to other materials and nanoparticles for the design of new cell-based assays and renewable microarray platforms.[23]

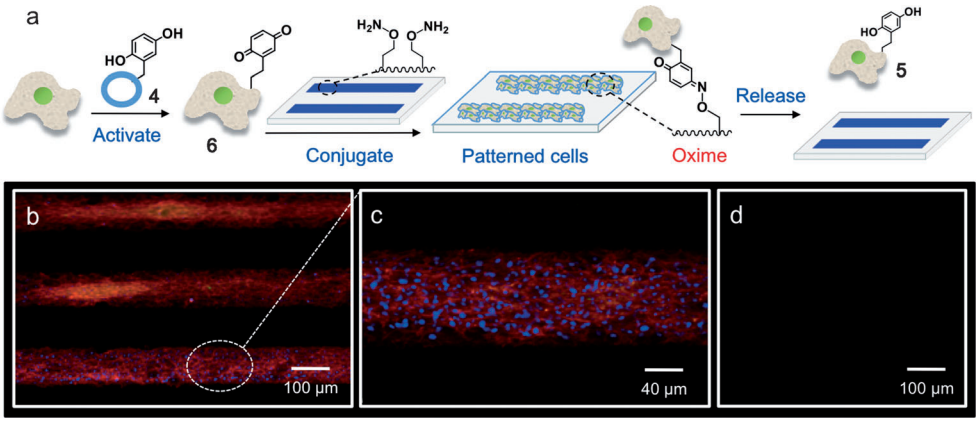

Figure 3. Fluorescence characterization of cyclical cell-surface tailoring and the release of ligands on the basis of redox-responsive chemoselective chemistry. a) Fbs were cultured with HQ-containing liposomes **4**, thus resulting in the membrane display of HQ on cell surfaces (cells **5**). Mild chemical oxidation converts HQ into Q groups on the cell surface (in **6**). Q-presenting Fbs **6** (10^4 cells mL^{-1}, 2 h) were then added to a substrate patterned with AO-terminated ligands. Cells adhered to the substrate owing to a biospecific interfacial oxime ligation and then proliferated within the patterned region, as shown by fluorescence microscopy at b) lower and c) higher magnification. Upon electrochemical reduction, the interfacial oxime is cleaved, and the cells are released from the substrate (d). Cells were stained for actin (red, phalloidin), the nucleus (blue, DAPI), and anti-vinculin (green, Cy-2).

We extended this methodology to demonstrate dynamic control over cell–cell interactions by coculturing HQ-presenting human mesenchymal stem cells (hMSCs) **13** with AO-displaying Fbs **15** to form 3D tissue structures. Upon chemical activation (see the Supporting Information) and mixing in solution, 3D spheroid assemblies could be rapidly generated (Figure 4a). By increasing the mixing duration, control of the spheroid size was possible (see Figure S12). The interconnected cells that make up the spheroids could then be disassembled into individual cells by mild electrochemical reduction (−100 mV, 10 s; Figure 4d). Additionally, spheroids were formed when Swiss 3T3 albino mouse Fbs presenting HQ groups were activated to **6** and cocultured with nuclear-mCherry-labeled Rat2 Fbs **14** displaying AO groups (Figure 4c). Figure 4e exhibits a cryo scanning electron micrograph (SEM) of an oxime-ligated, spheroid assembly of hMSCs (**11**) and Fbs (**14**) attached to a substrate. The viability of the cells in the spheroids was analyzed over time (1–5 h, trypan blue assay, blue false-colored) and found to be above 99% (see Figure S13). Control experiments without activation or when one of the oxime complements is not present in a cell type showed no spheroid formation. These results indicate that 3D coculture assemblies in solution can be generated in a straightforward manner with the ability to control both the size and composition of the assembly, as well as the duration of cell–cell interactions. This strategy is general and may be used for numerous studies, including autocrine and paracrine signaling events, and can be combined with microfabricated scaffolds as a tissue-engineering platform.

In addition to the formation of spheroid assemblies, we demonstrated that 3D multilayered coculture tissue structures can be generated on a solid support. We cultured activated, Q-presenting hMSCs **11** on a substrate to form a 2D monolayer (Figure 4e,f) and then added AO-displaying Fbs **15**. Chemoselective ligation occurred between the two cell populations, followed by 3D multilayer tissue growth after 3 days (Figure 4h). When the proper oxime pair was not present, only a single monolayer of hMSCs was observed, with no Fbs adhering. We found that cells were viable for many days (>7 days; see Figure S12) and that the HQ and AO groups could be carried forward on the cell surface (FACS analysis over time; see Figure S8), even through cell growth and proliferation. The multilayers could be disassembled by applying a mild reductive potential to the substrate (−100 mV, 10 s, pH 7.4) to cleave the oxime linkage and release the interactions between cells. Overall, this dynamic method to generate 3D multilayer tissue structures may be used to control cell–cell interactions for many coculture-based cell-behavioral and cell-tissue applications.[24]

We further employed this dynamic strategy to study stem-cell differentiation by applying our liposome-fusion-based delivery of activatable bioorthogonal groups to cell surfaces to generate 3D multilayered cell tissues and induce adipocyte differentiation (Figure 5). HQ-presenting hMSCs were activated and cocultured with Fbs as described previously. This tissue was grown in media that induced adipocyte differentiation after 10 days, thus resulting in 3D multilayered coculture tissues of adipocytes and Fbs (Figure 5d). The application of a mild reductive potential disassembled the 3D tissue after mild agitation to leave a relatively pure, 2D adipocyte monolayer (Figure 5e,f). The dynamic and con-

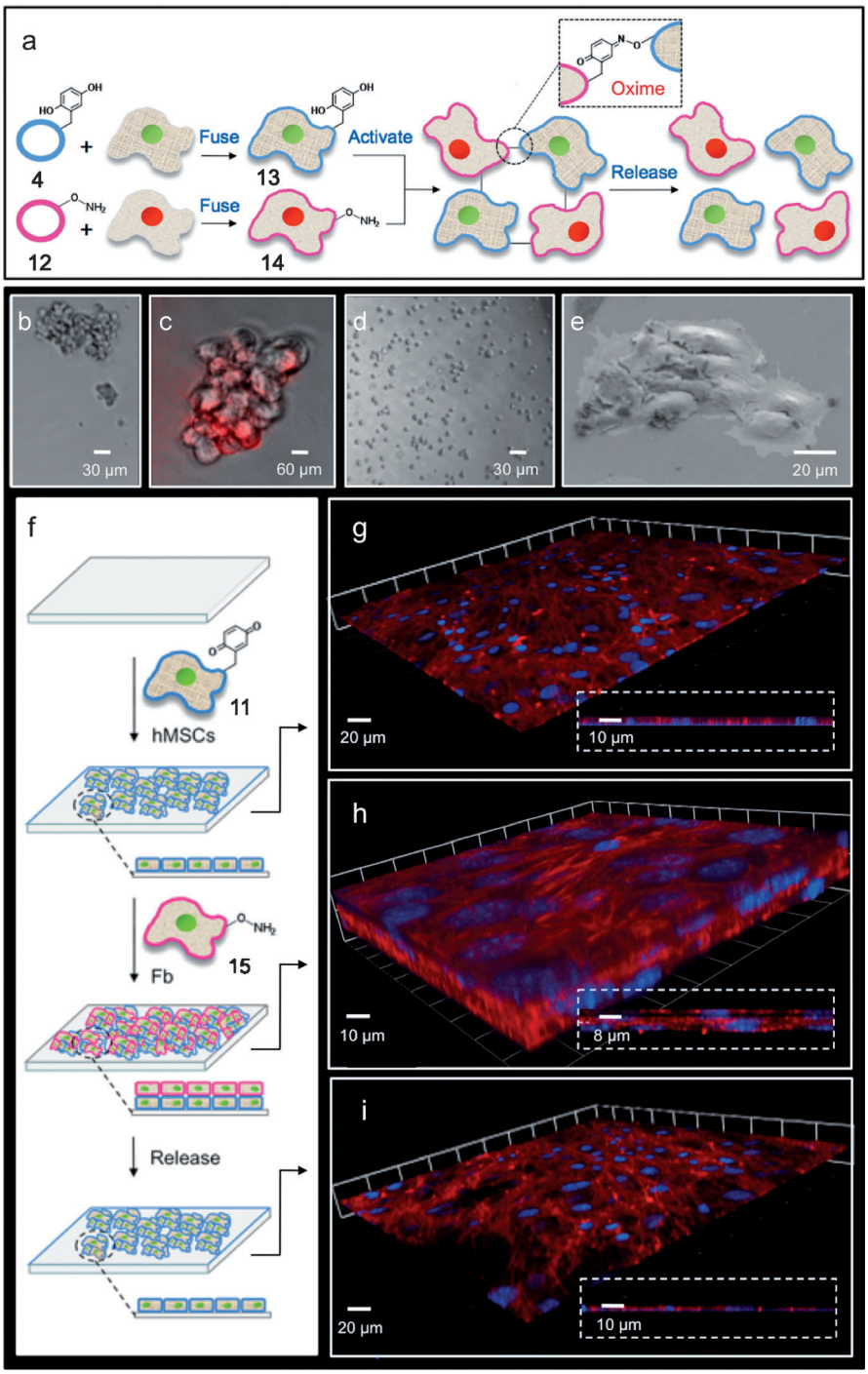

Figure 4. Scheme and corresponding images showing 3D dynamic spheroid and multilayered-tissue assembly and disassembly through liposome fusion and chemoselective cell-surface tailoring. a) Human mesenchymal stem cells (hMSCs) are functionalized with HQ groups to give **13** upon liposome fusion and are then activated to Q-functionalized hMSCs **11**. Fbs **14** presenting AO groups are then cocultured with Q-displaying hMSCs **11** to produce 3D spheroid assemblies (b, c, and e) through chemoselective oxime formation. Mild electrochemical reduction causes oxime cleavage and the dynamic disassembly of cells (d). f) Activated, Q-tethered hMSCs **11** are cultured on a substrate (10^5 cells mL^{-1}) to give a 2D cell monolayer (g). When AO-presenting Fbs **15** are added (10^5 cells mL^{-1}) to hMSCs **11**, a 3D interconnected multilayered structure forms (h). A reductive potential applied to the substrate cleaves the oxime bond and induces the dynamic release of Fbs from the multilayer, thus regenerating the 2D monolayer of hMSCs (i). The nuclei of AO-tethered Fbs **14** shown in (c) were stained with mCherry for enhanced visualization. The HMSCs **11** and Fbs **15** displayed in (g–i) were stained for actin (red, phalloidin) and the nucleus (blue, DAPI).

trolled 3D multilayer cell disassembly indicates that cell–cell interactions, even for complex stem-cell-differentiation processes over long time periods, can be precisely manipulated. By the assembly and disassembly of the cocultures on demand, a time course of cell behavior, owing to the length of cell–cell interactions, can be determined for a range of cell lines and coculture-based applications.[25]

In summary, we have developed a new general and straightforward liposome-based methodology for the delivery of dynamic and switchable bioorthogonal chemical functionalities to tailor cell membranes and direct the formation of 3D coculture tissue structures. We demonstrated and extensively characterized the conjugation and release of molecules to and from cell surfaces in situ, as well as the triggered assembly and disassembly of 3D spheroid and multilayered tissues. Additionally, dynamic cocultures of hMSCs and Fbs were able to be generated and differentiated by this redox oxime strategy.

The dynamic and bioorthogonal oxime chemistry reported has several key advantages as a cell-surface-engineering and cell-tissue-generating system. First, the oxime complementary pair is synthetically straightforward, and ketone-, hydrazide-, and AO-tethered ligands are commercially available. Second, oxime reactivity can be switched "on" and "off" through a change in the redox environment and can therefore be used to monitor the cell-surface incorporation of molecules and cell-surface interactions. Third, the oxime bond forms rapidly and is stable under physiological conditions until subjected to a chemical or electrochemical reducing potential. Fourth, the redox manipulation is noncytotoxic. Fifth, this liposome-fusion-based method is general and can be used to deliver the oxime pair to a range of cell lines for a variety of applications. This methodology can be used to deliver a variety of other bioorthogonal "click" functionalities to cell surfaces. Finally, by tailoring and controlling cell surfaces and cell–cell interactions, new types of autocrine and paracrine signaling studies for fundamental cell-behavio-

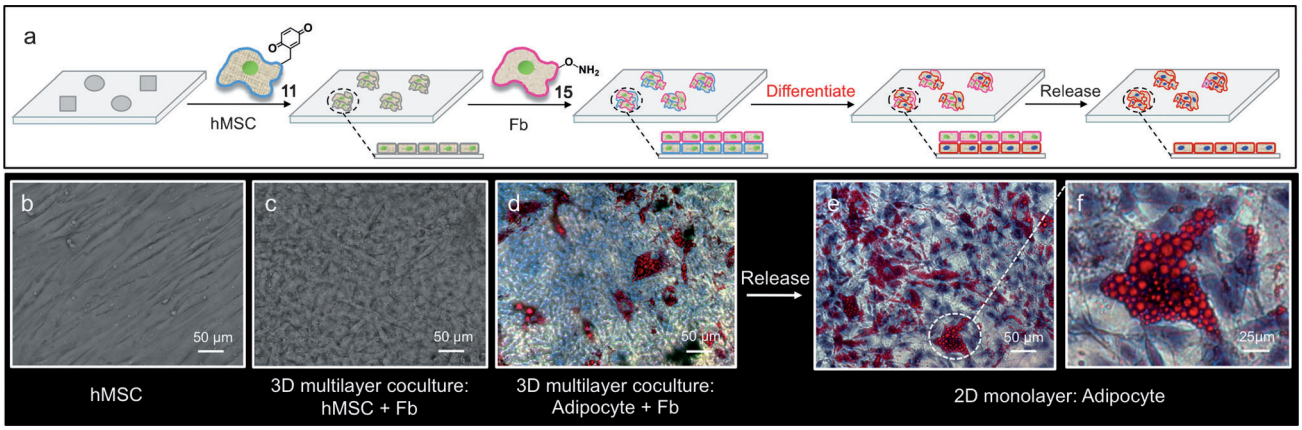

Figure 5. Scheme and corresponding phase-contrast images showing the formation, differentiation, and release of 3D dynamic tissues by the use of a Fb/hMSC coculture. a) Activated, Q-tethered hMSCs **11** are cultured on a substrate (10^5 cells mL^{-1}) and form a 2D monolayer, as shown by the image in (b). AO-presenting Fbs **15** are then added (10^5 cells mL^{-1}) to produce a 3D multilayered, interconnected coculture (c). When the appropriate induction medium is delivered to the coculture, hMSCs differentiate into adipocytes, thus resulting in a 3D multilayered coculture of Fbs and adipocytes (d). The dynamic release of Fbs leaves only the adhered adipocytes on the surface as a 2D monolayer, as shown by images at lower (e) and higher magnification (f). Adipocytes were stained for lipid vacuoles (red, Oil Red O) and the nucleus (purple, Harris hemotoxylin).

rial studies and tissue-regeneration applications may be explored.

Received: April 8, 2014
Published online: July 7, 2014

Keywords: cell-surface engineering · electrochemical oxidation · electrochemical reduction · liposomes · smart surfaces

[1] C. M. Nelson, M. J. Bissell, *Annu. Rev. Cell Dev. Biol.* **2006**, *22*, 287–291.
[2] L. Li, T. Xie, *Annu. Rev. Cell Dev. Biol.* **2005**, *21*, 605–612.
[3] a) A. S. Meshel, Q. Wei, R. S. Adelstein, M. P. Sheetz, *Nat. Cell Biol.* **2005**, *7*, 157–160; b) A. Engler, S. Sen, H. L. Sweeney, D. E. Discher, *Cell* **2006**, *126*, 677–683.
[4] S. F. Badylak, R. M. Nareem, *Proc. Natl. Acad. Sci. USA* **2010**, *107*, 3285–3288.
[5] a) Y. Ibold, S. Frauenschuh, C. Kaps, M. Sittinger, J. Ringe, P. M. Goetz, *J. Biomol. Screening* **2007**, *12*, 956–960; b) Y. Geng, P. Dalhaimer, S. Cai, R. Tsai, M. Tewari, D. E. Discher, *Nat. Nanotechnol.* **2007**, *2*, 249–255.
[6] D. R. Albrecht, G. H. Underhill, T. B. Wassermann, R. L. Sah, S. N. Bhatia, *Nat. Methods* **2006**, *3*, 369–374.
[7] W. R. Legant, A. Pathak, M. T. Yang, V. S. Deshpande, R. M. MacMeeking, C. S. Chen, *Proc. Natl. Acad. Sci. USA* **2009**, *106*, 10097–10103.
[8] a) A. M. Kloxin, A. M. Kasko, C. N. Salinas, K. S. Anseth, *Science* **2009**, *324*, 59–63; b) M. P. Lutolf, J. A. Hubbell, *Nat. Biotechnol.* **2005**, *23*, 47–55.
[9] a) S. Rasi Ghaemi, F. Harding, B. Delalat, R. Vasani, N. H. Voelcker, *Biomacromolecules* **2013**, *14*, 2675–2683; b) D. Falconnet, G. Csucs, H. M. Grandin, M. Textor, *Biomaterials* **2006**, *27*, 3044–3063; c) A. Khademhosseini, R. Langer, J. Borenstein, J. P. Vacanti, *Proc. Natl. Acad. Sci. USA* **2006**, *103*, 2480–2487.
[10] a) I. Drachuk, M. K. Gupta, V. V. Tsukruk, *Adv. Funct. Mater.* **2013**, *23*, 4437–4453; b) Z. J. Gartner, C. R. Bertozzi, *Proc. Natl. Acad. Sci. USA* **2009**, *106*, 4606–4610.
[11] L. K. Mahal, K. J. Yarema, C. R. Bertozzi, *Science* **1997**, *276*, 1125–1128.
[12] N. C. Yoder, D. Yuksel, L. Dafik, K. Kumar, *Curr. Opin. Chem. Biol.* **2006**, *10*, 576–583.
[13] R. S. Raghavan, H. C. Hang, *Drug Discovery Today* **2009**, *14*, 178–184.
[14] M. D. Best, *Biochemistry* **2009**, *48*, 6571–6584.
[15] E. Saxon, C. R. Bertozzi, *Science* **2000**, *287*, 2007–2010.
[16] a) Y. Gong, Y. Luo, D. Bong, *J. Am. Chem. Soc.* **2006**, *128*, 14430–14431; b) J. Lee, H. Jun, J. Kim, *Adv. Mater.* **2009**, *21*, 3674–3678.
[17] a) H. R. Zope, F. Versluis, A. Ordas, J. Voskuhl, H. P. Spaink, A. Kros, *Angew. Chem.* **2013**, *125*, 14497–14501; *Angew. Chem. Int. Ed.* **2013**, *52*, 14247–14251; b) Q. Saleem, Z. F. Zhang, C. C. Gradinaru, P. M. Macdonald, *Langmuir* **2013**, *29*, 14603–14612; c) D. Sarkar, P. K. Vemula, W. Zhao, A. Gupta, R. Karnik, J. M. Karp, *Biomaterials* **2010**, *31*, 5266–5274.
[18] a) S. Park, N. Westcott, W. Luo, D. Dutta, M. N. Yousaf, *Bioconjugate Chem.* **2014**, *25*, 543–551; b) D. Dutta, A. Pulsipher, M. N. Yousaf, *Langmuir* **2010**, *26*, 9835–9841; c) E. W. L. Chan, S. Park, M. N. Yousaf, *Angew. Chem.* **2008**, *120*, 6363–6367; *Angew. Chem. Int. Ed.* **2008**, *47*, 6267–6271.
[19] E. W. L. Chan, M. N. Yousaf, *J. Am. Chem. Soc.* **2006**, *128*, 15542–15546.
[20] a) J. Fuchs, S. Böhme, F. Oswald, P. N. Hedde, M. Krause, J. Wiedenmann, G. U. Nienhaus, *Nat. Methods* **2010**, *7*, 627–630; b) M. Larsen, C. Wei, K. M. Yamada, *J. Cell Sci.* **2006**, *119*, 3376–3384.
[21] S. Park, M. N. Yousaf, *Langmuir* **2008**, *24*, 6201–6207.
[22] M. Mrksich, *ACS Nano* **2008**, *2*, 7–18.
[23] a) R. Karnik, S. Hong, H. Zhang, Y. Mei, D. Anderson, J. Karp, R. Langer, *Nano Lett.* **2008**, *8*, 1153–1158; b) S. R. Khetani, S. N. Bhatia, *Nat. Biotechnol.* **2008**, *26*, 120–126.
[24] R. Inaba, A. Khademhosseini, H. Suzuki, J. Fukuda, *Biomaterials* **2009**, *30*, 3573–3579.
[25] L. Gan, R. A. Kandel, *Tissue Eng.* **2007**, *13*, 831–842.